Biochemical and Biophysical Research Communications 441 (2013) 493–498

Contents lists available at ScienceDirect

Biochemical and Biophysical Research Communications

journal homepage: www.elsevier.com/locate/ybbrc

Site-specific aspartic acid isomerization regulates self-assembly and neurotoxicity of amyloid-β

Toshihiko Sugiki [a], Naoko Utsunomiya-Tate [a,b,*]

[a] Laboratory of Physical Chemistry, Research Institute of Pharmaceutical Sciences, Musashino University, Japan
[b] Laboratory of Basic Chemistry and Molecular Structure, Faculty of Pharma Sciences, Teikyo University, Japan

ARTICLE INFO

Article history:
Received 9 October 2013
Available online 25 October 2013

Keywords:
Amyloid-β
$A\beta_{1-42}$
Alzheimer's diseases
D-Asp isomerization
Circular dichroism

ABSTRACT

Amyloid-β (Aβ) proteins, which consist of 42 amino acids ($A\beta_{1-42}$), are the major constituent of neuritic plaques that form in the brains of senile patients with Alzheimer's disease (AD). Several reports state that three aspartic acid (Asp) residues at positions 1, 7, and 23 in $A\beta_{1-42}$ in the plaques of patients with AD are highly isomerized from the L- to D-form. Using biophysical experiments, the present study shows that simultaneous D-isomerization of Asp residues at positions 7 and 23 (D-$Asp^{7,23}$) enhances oligomerization, fibril formation, and neurotoxic effect of $A\beta_{1-42}$. In addition, D-isomerization of Asp at position 1 (D-Asp^{1}) suppresses malignant effects induced by D-$Asp^{7,23}$ of $A\beta_{1-42}$. These results provide fundamental information to elucidate molecular mechanisms of AD pathogenesis and to develop potent inhibitors of amyloid aggregates and Aβ neurotoxicity.

1. Introduction

Amyloid-β (Aβ) fibrillation is accelerated by age- and stress-dependent modulations of its structural conformation and solubility. Insoluble higher-order assemblies of Aβ peptides are abundantly found in plaques in the brains of senile patients with Alzheimers disease (AD) [1–3]. Although Aβ is associated with AD pathology, the biological function of Aβ and the mechanisms of how Aβ leads to amyloidosis remain unclear. In the brain tissue, two types of Aβ peptides are generated by proteolytic cleavage of the precursor protein, which consist of 40 and 42 amino acids, respectively. Because the latter Aβ peptide ($A\beta_{1-42}$) has lower solubility and higher neurotoxicity than the former ($A\beta_{1-40}$) and is the major constituent of plaques of patients with AD, $A\beta_{1-42}$ is primarily associated with AD pathology [3]. Aβ peptides initially fold into antiparallel β-turn–β topology, and then intermolecular hydrophobic packing between the β-strands generates protofibrils. The orderly stacked Aβ protofibrils become a seed for the more mature fibril that generates larger aggregates by forming "cross-β" structures, in which each parallel β-strand is oriented to the axis of the fibril [4].

Proteins are *de novo* synthesized using only L-amino acids. However, due to aging, proteins containing D-isomerized Asp (D-Asp) residues progressively increase in numerous tissues [5]. D-Isomerization of amino acids is one of the age-dependent post-translational modifications, and it is the most common type of aging-related protein damage [6]. D-Isomerization spontaneously and nonenzymatically progresses under physiological conditions [5]. Because isomerization introduces additional methylene groups into the protein backbone moiety, isomerization of amino acid residues leads to considerable changes in physical properties, such as solubility and alterations in protein conformation, and it may cause abnormal protein accumulation in human tissues [5,7]. The wild-type Aβ has three L-Asp residues at positions 1, 7, and 23. Asp residues within Aβ are highly isomerized from the L- to the D-form in plaques in the brains of senile patients with AD [8,9]. In addition, several studies show that the aggregation ability of $A\beta_{1-42}$ is enhanced by D-isomerization of Asp residues [10,11]. Therefore, quantitative detection of D-Asp-isomerized $A\beta_{1-42}$ is important for accurate clinical diagnosis of AD. Furthermore, analyses of physicochemical characteristics and neurotoxicity of D-Asp-isomerized $A\beta_{1-42}$ by biophysical experiments are essential to elucidate molecular mechanisms of AD pathology. In addition, elucidation of structural features of proteins containing D-isomerized amino acids and their relationship with pathogenesis of senile diseases is important in the development of new effective drugs. However, these mechanisms remain unclear.

In this study, we investigated the effect of D-isomerization of Asp residues in $A\beta_{1-42}$ on its oligomerization and fibrillation pro-

Abbreviations: Aβ, amyloid-β; Asp, aspartic acid; ANS, 1-anilinonaphthalene-8-sulfonic acid; Bis-ANS, 4,4′-dianilino-1,1′-binaphthyl-5,5′-disulfonic acid; CD, circular dichroism; MTT, 3-(4,5-dimethylthiazol-2-yl)-2,5-diphenyltetrazolium bromide; ThT, thioflavin-T; PICUP, photo-induced cross-linking of unmodified proteins.

* Corresponding author at: Teikyo University, 2-11-1 Kaga, Itabashi-ku, Tokyo 173-8605, Japan. Fax: +81 3 3964 8025.

0006-291X/$ - see front matter © 2013 Elsevier Inc. All rights reserved.
http://dx.doi.org/10.1016/j.bbrc.2013.10.084

files, and calculated the correlation between the physicochemical characters of D-Asp-substituted $A\beta_{1-42}$ and neurotoxicity. We found that simultaneous D-isomerization of Asp^7 and Asp^{23} ($D\text{-}Asp^{7,23}$) markedly accelerates $A\beta_{1-42}$ fibrillation compared with that of the wild type, and its neurotoxicity is clearly correlated with its fibrillation characteristics. Furthermore, it was revealed that D-isomerization of Asp^1 significantly suppresses the malignant effect caused by $D\text{-}Asp^{7,23}$. In this study, we found that solubility and fibrillation characteristics of $A\beta_{1-42}$ are finely regulated by site-specific D-isomerization of Asp residues, and individual roles of each Asp residue as a trigger or inhibitor of fibrillation and neurotoxicity of $A\beta_{1-42}$ could be clearly identified.

2. Materials and methods

2.1. Materials

$A\beta_{1-42}$ and other D-isomers ([$D\text{-}Asp^{23}$], [$D\text{-}Asp^{1,23}$], [$D\text{-}Asp^{7,23}$], and [$D\text{-}Asp^{1,7,23}$] $A\beta_{1-42}$) were purchased from AnyGen Co., Ltd., and their solutions were prepared as described previously [11]. Rat pheochromocytoma PC-12 cells were purchased from Riken Cell Bank. The anti-$A\beta_{17-24}$ mouse monoclonal antibody 4G8 and horseradish peroxidase-linked anti-mouse IgG antibody were purchased from Covance and GE healthcare, respectively. All other chemical materials used in this study were purchased from Wako, Nacalai Tesque, Inc., and GE healthcare.

2.2. CD spectroscopy

Far-UV CD spectra of $A\beta_{1-42}$ were measured using a J-820 spectrometer (JASCO), and molar ellipticities were calculated as described previously [11,12]. Based on the molar ellipticity values, deconvolutions of content of secondary structures (α-helix, β-sheet, turn, and random coil) were performed using the program Reed's algorithm, which was supplied by JASCO [13].

2.3. Photochemical cross-linking of $A\beta_{1-42}$ and Western blotting

A solution of $A\beta_{1-42}$ (20 μM) was incubated at 37 °C for 7 h, and $A\beta_{1-42}$ oligomers were stabilized by the PICUP method, as described previously [14–16]. A 60-W filament lamp was used as an optical source and exposure time was 7 s. Oligomers were separated by SDS Tricine–PAGE and transferred to PVDF membranes; size distribution of the oligomers was analyzed by Western blotting using the anti-Aβ antibody 4G8.

2.4. 1-Anilinonaphthalene-8-sulfonic acid (ANS) fluorescence measurement

$A\beta_{1-42}$ was dissolved in 50 mM sodium phosphate buffer (pH 7.4) to a final concentration of 20 μM. Following the desired incubation periods, protein stock solutions were diluted to a final concentration of 1 μM in 50 mM sodium phosphate buffer (pH 7.4) containing 20 μM of 4,4′-dianilino-1,1′-binaphthyl-5,5′-disulfonic acid (bis-ANS). Fluorescence of bis-ANS was excited at 350 nm in a quartz cuvette with a 10-mm light path gap, and its emission spectra in the 400–650-nm range were recorded using a RF-5300 fluorometer (SHIMADZU) at a steady room temperature.

2.5. ThT binding assay

$A\beta_{1-42}$ fibrils were quantitatively evaluated by the ThT binding assay as described previously [11].

2.6. MTT assay

PC-12 cells were cultured in D-MEM, plated in a poly-L-lysine-coated 24-wells plate at a density of 4×10^4 cells/mL, and treated with 50 pg/mL of a nerve growth factor (NGF) for 48 h. $A\beta_{1-42}$ solutions (20 μM) were preincubated at 37 °C for 24 h; subsequently, the differentiated cells were coincubated with fresh media containing 5 μM of $A\beta_{1-42}$ peptides for another 12 h. Thereafter, 20 μL/well of 5 mg/mL MTT solution was added to the PC-12 cells and incubated at 37 °C for 1 h. The chromogenic reaction was stopped by adding 20 μL/well of 0.1 M HCl, and the absorbance of visible light at 540 nm was measured. All the absorbance data were subtracted by reference data, which was measured at 650 nm. The ratio of MTT reduction was shown as the fold difference of the blank ± S.E.M. from five representative results of multiple independent experiments. Statistical analyses were performed using Tukey's test. A P-value of<0.05 was considered to be significant.

3. Results

3.1. β-Sheet formation of D-Asp-containing $A\beta_{1-42}$ protein

Structural features of the wild-type $A\beta_{1-42}$ and its analogs, in which three L-Asp were substituted with D-Asp at positions 1, 7, and 23 in several combinations, were analyzed by measuring their CD spectra. Kinetic rates of β-sheet formation of wild-type and D-Asp-containing $A\beta_{1-42}$ proteins were estimated from incubation period-dependent increments of molar ellipticity at 218 nm (Fig. 1 and Table 1). In addition, the CD spectra were deconvoluted to evaluate alterations in secondary structure contents (Table 2). As a result, the β-sheet formation rates of D-Asp-containing $A\beta_{1-42}$ proteins increased by 2 to 3-fold compared with those of wild-type $A\beta_{1-42}$ (Table 1). With regard to $D\text{-}Asp^{7,23}$ isomerization, the β-sheet formation rate was extremely prompt, with the β-sheet forming prior to the start of incubation (Fig. 1A).

3.2. Oligomerization profiles of the D-Asp-containing $A\beta_{1-42}$ proteins

Oligomerization properties of D-Asp-containing $A\beta_{1-42}$ proteins were evaluated by a combination of photochemical cross-linking methods and Western blotting. Using the indicated experimental conditions, $A\beta_{1-42}$ oligomerization was visually confirmed (Fig. 2A). Several interesting oligomerization characteristics were seen in the case of [$D\text{-}Asp^{7,23}$] $A\beta_{1-42}$. The most abundant oligomeric components in [$D\text{-}Asp^{7,23}$] $A\beta_{1-42}$ were tetramers, whereas the major oligomeric components of $A\beta_{1-42}$ were primarily pentamers and hexamers (Fig. 2A). To further investigate the differences in oligomerization states of each $A\beta_{1-42}$ protein, we performed ANS binding assays using bis-ANS as a probe (Fig. 2B). Because bis-ANS preferentially binds to the solvent-exposed hydrophobic crevices, which are present on protein surfaces, resulting in a significant increase of its quantum yield, it is commonly used as a sensitive indicator of partially unfolded and intermediate structural states of proteins [17]. Bis-ANS, a probe for oligomeric intermediate assemblies of Aβ, is frequently used to detect and analyze formation kinetics of oligomerization and prefibrillar states of $A\beta_{1-42}$ [18]. As a result, fluorescence intensities of bis-ANS were gradually attenuated in an incubation time-dependent manner (Fig. 2B). Because bis-ANS selectively recognizes a relatively small size of oligomeric intermediate assemblies, which were detected by the photochemical cross-linking method, it indicates that the quantity of $A\beta_{1-42}$–ANS binding decreased by degrees according to the morphological transition from the oligomeric state to matured fibril. It was revealed that the attenuation rates of bis-ANS binding

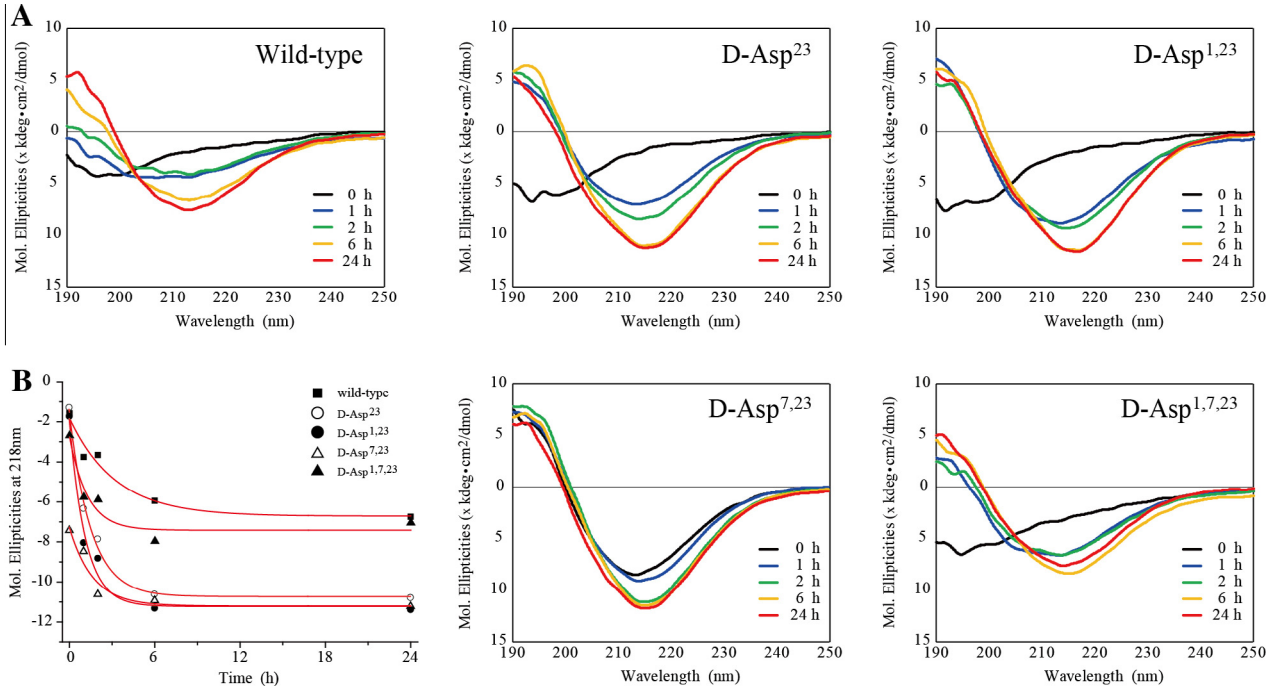

Fig. 1. Time-dependent conformational change in $A\beta_{1-42}$ peptides (A) CD spectra of the wild-type and D-Asp-substituted $A\beta_{1-42}$. From the start point of incubation at 37 °C, far-UV CD spectra (wavelength 190–250 nm) were measured at the following time points (0, 1, 2, 6, and 24 h). (B) Comparison of time-dependent increases in molar ellipticities at 218 nm. Kinetic rates of β-sheet formation of all D-Asp-substituted $A\beta_{1-42}$ were estimated by measuring incubation period (37 °C)-dependent alterations of molecular ellipticities at a CD spectra of 218 nm. All the plots were fitted by the single-exponential decay equation (red solid lines), and the time constants (k) of β-sheet formation were determined as described in Table 1.

Table 1
Kinetic rate coefficients of β-sheet formation of $A\beta_{1-42}$ peptides.

$A\beta_{1-42}$	k (h^{-1})	Fold increase
Wild type	0.31 ± 0.11	1.00
D-Asp^{23}	0.66 ± 0.08	2.13
D-$Asp^{1,23}$	0.88 ± 0.20	2.84
D-$Asp^{7,23}$	0.61 ± 0.27	1.97
D-$Asp^{1,7,23}$	0.79 ± 0.35	2.55

Table 2
Time-course analyses of composition of $A\beta_{1-42}$ secondary structures.

$A\beta_{1-42}$		Incubation periods (h)				
		0	1	2	6	24
Wild type	α-Helix	0	0	0	1.9	2.6
	β-Sheet	38.8	48.3	49.2	49.2	45.5
	Turn	0	0	0	2.5	6.9
	Random	61.2	51.7	49.9	46.4	45.0
D-Asp^{23}	α-Helix	0	1.9	2.0	0.8	0.3
	β-Sheet	33.1	46.8	48.2	54.6	54.3
	Turn	0	6.2	5.0	1.0	0
	Random	66.9	45.1	44.8	43.6	45.4
D-$Asp^{1,23}$	α-Helix	0	4.5	0.9	0	0.1
	β-Sheet	33.1	45.1	51.5	56.3	55.3
	Turn	0	4.8	2.3	0	0
	Random	66.9	45.5	45.3	43.7	44.6
D-$Asp^{7,23}$	α-Helix	2.0	1.5	0.5	0.2	0.2
	β-Sheet	46.1	49.7	55.3	56.4	54.8
	Turn	7.8	5.6	2.1	0.7	0.8
	Random	44.1	43.2	42.1	42.7	44.2
D-$Asp^{1,7,23}$	α-Helix	0	1.6	0	0.1	1.8
	β-Sheet	39.6	44.6	49.6	55.4	49.3
	Turn	0	5.8	3.4	0	3.9
	Random	60.4	47.9	47.0	44.6	45.0

quantities of [D-Asp^{23}] and [D-$Asp^{7,23}$] $A\beta_{1-42}$ were faster compared with those of [D-$Asp^{1,23}$] and [D-$Asp^{1,7,23}$] $A\beta_{1-42}$ (Fig. 2B). These data revealed that the kinetic rate of $A\beta_{1-42}$ structural change from oligomer to fibril could be enhanced by D-Asp^{23} and D-$Asp^{7,23}$ substitutions.

3.3. Fibrillation of D-Asp-containing $A\beta_{1-42}$ proteins

Fibrillation levels of various D-Asp-containing $A\beta_{1-42}$ proteins were evaluated by the ThT binding assay because ThT selectively binds to mature fibrils rather than immature molecular assemblies, prominently increasing its fluorescence intensity [19,20]. As a result of the ThT binding assay, fluorescence intensities in all $A\beta_{1-42}$ types reached a plateau at 12 h after the start of incubation. Moreover, [D-$Asp^{7,23}$] $A\beta_{1-42}$ exhibited a drastic increase in the ThT fluorescence intensity, and a considerable quantity of mature fibrils were already formed at the initial incubation time (Fig. 2C). Furthermore, the ThT binding quantity of [D-$Asp^{1,7,23}$] $A\beta_{1-42}$, which adds an additional D-Asp^{1} isomerization on D-$Asp^{7,23}$, was not elevated, such as that in [D-$Asp^{7,23}$] $A\beta_{1-42}$ (Fig. 2C).

3.4. Correlation between structural features and neurotoxicities of D-Asp-containing $A\beta_{1-42}$ proteins

Neurotoxicities of various D-Asp-containing $A\beta_{1-42}$ proteins were evaluated by the MTT assay. As a result, [D-$Asp^{7,23}$] $A\beta_{1-42}$ has neurotoxicity more severe than the wild type (Fig. 3). Moreover, neurotoxicities of [D-$Asp^{1,23}$] and [D-$Asp^{7,23}$] $A\beta_{1-42}$ were comparable to the that of the wild type, and were significantly lower than that of [D-$Asp^{7,23}$] $A\beta_{1-42}$ (Fig. 3). Based on these results, we further investigated the relationship between the morphological changes of these D-Asp-isomerized $A\beta_{1-42}$ and their degrees of neurotoxicity. A positive correlation between the ThT-binding quantity and the neurotoxicity of D-Asp-isomerized $A\beta_{1-42}$ pep-

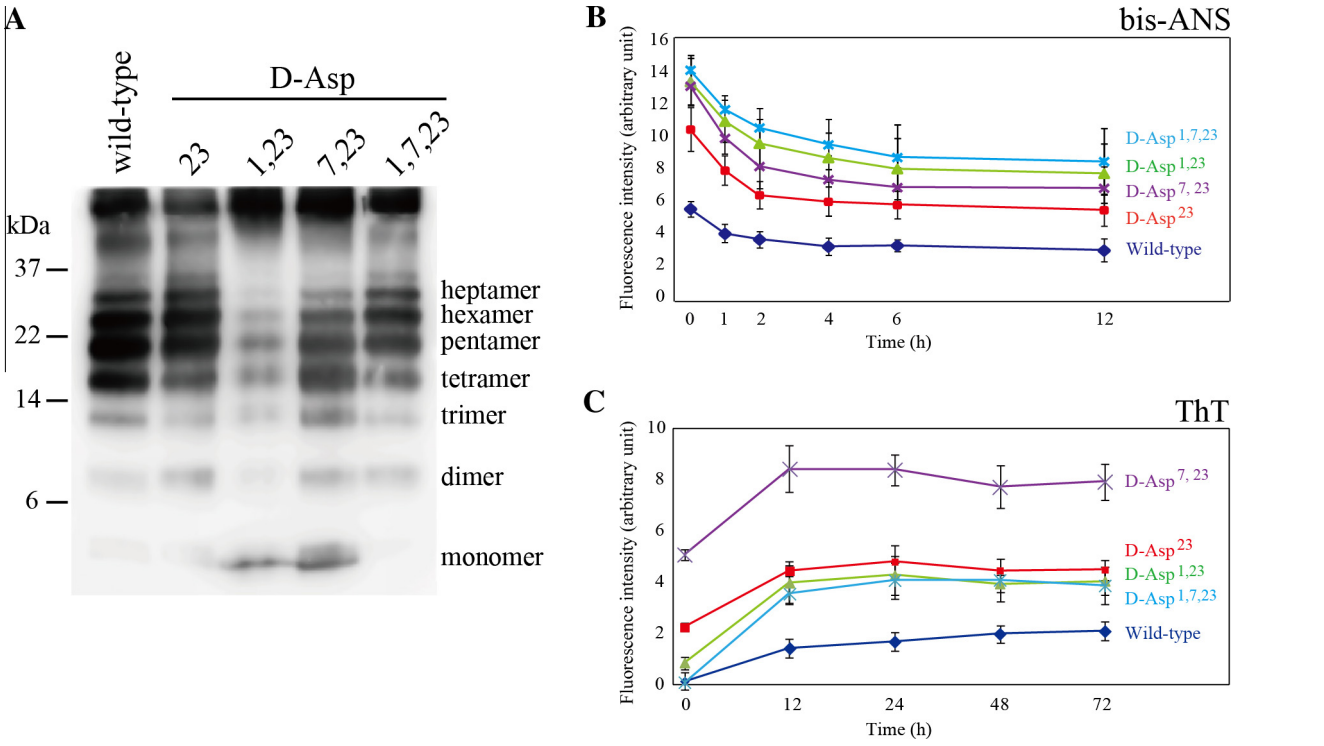

Fig. 2. (A) Oligomer size distribution of $A\beta_{1-42}$ assessed by PICUP method and Western blotting. (B and C) Analyses of oligomerization and fibrillation profiles of D-Asp-substituted $A\beta_{1-42}$ by performing ANS- and ThT-binding assays, respectively. Plots display time-dependent increments of (B) $A\beta_{1-42}$–ANS binding or (C) $A\beta_{1-42}$–ThT binding quantities.

tides was clearly calculated (Fig. 4). In addition, it revealed that the correlation between the ANS-binding quantity and neurotoxicity of D-Asp-isomerized $A\beta_{1-42}$ peptides was extremely low (Fig. 4).

4. Discussion

In this study, differences in oligomerization or fibrillation degrees and neurotoxicities among various D-Asp-containing $A\beta_{1-42}$ proteins were analyzed by physicochemical and biochemical experiments. As a result, (1) kinetic rates of β-sheet formation of [D-Asp^{23}] and [D-$Asp^{7,23}$] $A\beta_{1-42}$ were approximately fold higher than those of the wild type (Fig. 1 and Table. 1). Furthermore, the morphological transition rate from oligomer to higher-order assemblies was accelerated by D-Asp^{23} and D-$Asp^{7,23}$ substitutions compared with that of the wild type and other D-form substituted $A\beta_{1-42}$ (Fig. 2B); (2) kinetic rates of β-sheet formation of [D-$Asp^{1,23}$] and [D-$Asp^{1,7,23}$] $A\beta_{1-42}$ were approximately threefold higher than those of the wild type (Fig. 1 and Table. 1). However, the morphological transition rate from oligomers to fibril states and their neurotoxicities were comparable to those of the wild type (Figs. 2 and 3); and (3) degrees of neurotoxicity of D-Asp-isomerized $A\beta_{1-42}$ highly correlated with their degrees of fibrillation maturity (Fig. 4).

Morphological and neurotoxic modes of [D-$Asp^{7,23}$] $A\beta_{1-42}$ were obviously more characteristic than those of all others. For example, β-sheet topology was formed prior to the start of incubation (Fig. 1A). This indicates that D-$Asp^{7,23}$ isomerization prominently enhances $A\beta_{1-42}$ β-sheet formation. Furthermore, maturation of the fibrillation state of $A\beta_{1-42}$ drastically increased by D-$Asp^{7,23}$ isomerization (Fig. 2C). These results demonstrate that D-$Asp^{7,23}$ isomerization gives severe fibrillation-prone characteristics to $A\beta_{1-42}$. In parallel with the structural characterizations, neurotoxicity of $A\beta_{1-42}$ increased by D-$Asp^{7,23}$ isomerization (Fig. 3).

On the other hand, the kinetic rates of oligomer–fibril transition and fibrillation maturity of [D-$Asp^{1,7,23}$] $A\beta_{1-42}$ were comparable to those of wild-type $A\beta_{1-42}$ (Fig. 2C). These results indicate that fibrillation-prone characteristics of $A\beta_{1-42}$ caused by D-$Asp^{7,23}$ isomerization were significantly suppressed by additional D-Asp^{1} isomerization. This may suggest that D-Asp^{1} isomerization plays a role in delaying the progression of morphological changes from β-sheets to higher-order oligomeric architectures and/or mature fibrils of the $A\beta_{1-42}$.

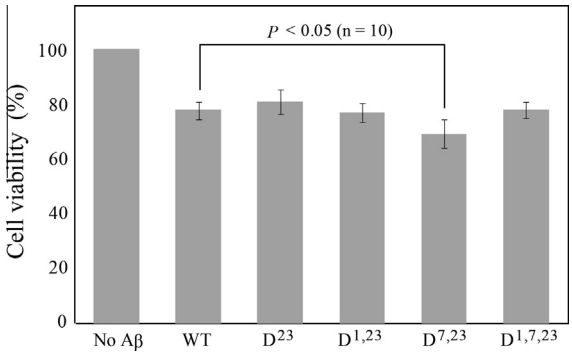

Fig. 3. Neurotoxicity of D-Asp-substituted $A\beta_{1-42}$. Significant differences in neurotoxicities among the D-Asp-substituted $A\beta_{1-42}$ proteins were assessed by performing *t*-tests on results from representative assays of at least five independent experiments.

Subsequently, we analyzed the neurotoxicity of each D-Asp-isomerized $A\beta_{1-42}$ by the MTT assay. As a result, it was elucidated that fibrillation-prone [D-$Asp^{7,23}$] $A\beta_{1-42}$ imparts more severe toxicity against neuronal cells compared with the wild type (Fig. 3). On the other hand, all other D-Asp-containing $A\beta_{1-42}$ proteins displayed neurotoxicities comparable to those of the wild type (Fig. 3). These results indicate that D-Asp^{1} isomerization not only significantly inhibits the $A\beta_{1-42}$ fibrillation enhancement effect caused by D-$Asp^{7,23}$ but also has the potential to block augmentation of neurotoxicity caused by D-$Asp^{7,23}$ isomerization.

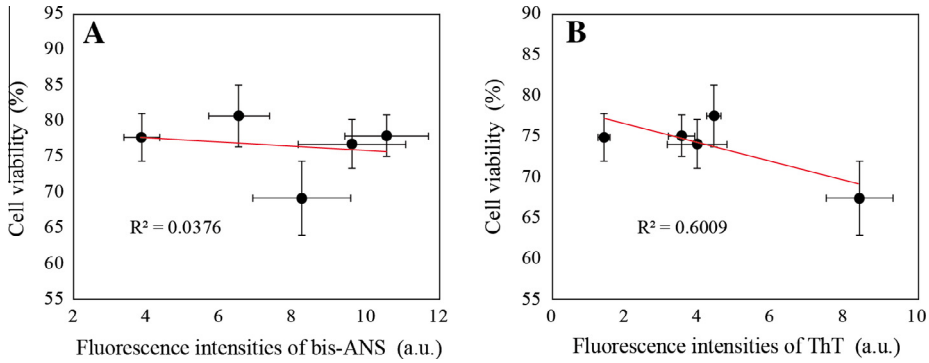

Fig. 4. Correlations between the oligomerization/aggregation/fibrillation profiles and neurotoxicity of D-Asp-substituted $A\beta_{1-42}$. Two-dimensional correlation plots of the increment in (A) ANS fluorescence signal intensity or (B) ThT binding quantities (as the horizontal axis, respectively) and the corresponding neurotoxicity (as the vertical axis) of each D-Asp-substituted $A\beta_{1-42}$.

Furthermore, correlation analyses indicate that the extent of neurotoxicity of each D-Asp-containing $A\beta_{1-42}$ proteins clearly correlates to fibril maturation levels rather than the levels of intermediate insoluble small aggregates (Fig. 4). In several cases, during morphological transition, intermediate structures, which are specifically detected by typical hydrophobic probes, such as bis-ANS, tend to form misfolded, immature structures, and/or are relatively heterologous insoluble aggregates. Accumulation of such structurally immature aggregates imparts strong neurotoxicity, leading to various neurodegenerative diseases [21]. Recently, several studies indicate that $A\beta_{1-42}$ oligomerization, which precedes fibrillation, conveys higher neurotoxicity than the fibril state [22,23]. However, in this study, D-isomerization of $Asp^{7,23}$, which causes significant progression of $A\beta_{1-42}$ fibrillation, showed severe neurotoxic effects compared with those caused by D-isomerization of $Asp^{1,23}$ and $Asp^{1,7,23}$. Based on these results, the augmentation of $A\beta_{1-42}$ neurotoxicity caused by D-$Asp^{7,23}$ isomerization is due to the presence of a mature fibril.

In contrast to D-$Asp^{7,23}$, the oligomerization level, higher-order morphology, and neurotoxicity of $A\beta_{1-42}$ were not drastically altered by the sole isomerization of Asp^{23} because both ANS- and ThT-binding quantities and neurotoxicity of [D-Asp^{23}] $A\beta_{1-42}$ were comparable to those of wild type. This result is consistent with a previous study [24], and our group similarly reported that the significant structural alteration in $A\beta_{1-42}$ cannot be caused by a single isomerization of Asp^{7} [11]. Based on previous reports and results of this study, single Asp^{23} isomerization may result in relatively small but indispensable structural alterations in $A\beta_{1-42}$. Asp^{23} residues play a significant role in shaping the turn structure connecting two β-strands in $A\beta_{1-42}$, and the stable turn formation augments fibrillation and neurotoxicity of $A\beta_{1-42}$ [25]. Furthermore, the turn structure of $A\beta_{1-42}$ has several different conformations, and minor "malignant" conformations of $A\beta_{1-42}$ are more thermodynamically stable, demonstrating fibrillation-prone qualities and severe neurotoxicity [25]. Although there are no significant structural differences in the turn region between the minor malignant and other conformations, orientation of the Asp^{23} side chain clearly differed [25]. In the case of major conformations, the side chain of Asp^{23} is oriented to the same side of the hydrophobic patch that exists on the antiparallel β-strands. On the other hand, in the case of the malignant minor conformation, the side chain of Asp^{23} is oriented in the direction opposite to that of the hydrophobic surface [25]. The malignant conformation-like structure can be generated by D-isomerization of Asp^{23}. Although the malignant conformation is minor, it could be a seed that generates mature fibrils, triggering growth and aggregation that eventually causes AD development [25]. Therefore, it is thought that single isomerization of Asp^{23} from the L- to D-form causes considerable structural perturbations, but it is insufficient to be a huge driving force that enables the drastic structural change of $A\beta_{1-42}$. However, significant structural alterations may be encouraged by further D-Asp^{7} isomerization on [D-Asp^{23}] $A\beta_{1-42}$.

In this study, we found that the solubility, morphological change, and neurotoxicity level of $A\beta_{1-42}$ are finely regulated by site-specific D-isomerization of three Asp residues. In addition, we identified "hot spot" Asp residues that accelerate or suppress fibrillation and neurotoxicity.

Although D-isomerization occurs spontaneously and nonenzymatically under physiological conditions, D-isomerized Asp could be repaired by protein isoaspartyl *O*-methyltransferase (PIMT), which converts D-isomerized Asp back to L-form [26]. It is possible that the collapse of balance between D-isomerization and stereochemical back-conversion of Asp residues observed in aging is one of the causes of senile AD [27]. In particular, increases in D-$Asp^{7,23}$ isomerization and/or decreases in D-Asp^{1} isomerization of $A\beta_{1-42}$ triggered by aging may lead to sickness in the brain.

References

[1] H. Braak, E. Braak, I. Grundke-Iqbal, K. Iqbal, Occurrence of neuropil threads in the senile human brain and in Alzheimer's disease: a third location of paired helical filaments outside of neurofibrillary tangles and neuritic plaques, Neurosci. Lett. 65 (1986) 351–355.

[2] V.W. Henderson, C.E. Finch, The neurobiology of Alzheimer's disease, J. Neurosurg. 70 (1989) 335–353.

[3] A.E. Roher, J.D. Lowenson, S. Clarke, A.S. Woods, R.J. Cotter, E. Gowing, M.J. Ball, β-Amyloid-(1–42) is a major component of cerebrovascular amyloid deposits: implications for the pathology of Alzheimer disease, Proc. Natl. Acad. Sci. USA 90 (1993) 10836–10840.

[4] J.J. Balbach, A.T. Petkova, N.A. Oyler, O.N. Antzutkin, D.J. Gordon, S.C. Meredith, R. Tycko, Supermolecular structure in full-length Alzheimer's β-amyloid fibrils: evidence for a parallel β-sheet organization from solid-state nuclear magnetic resonance, Biophys. J. 83 (2002) 1205–1216.

[5] S. Ritz-Timme, M.J. Collins, Racemization of aspartic acid in human protein, Ageing Res. Rev. 1 (2002) 43–59.

[6] J. Orpiszewski, M.D. Benson, Induction of beta-sheet structure in amyloidogenic peptides by neutralization of aspartate: a model for amyloid nucleation, J. Mol. Biol. 289 (1999) 413–428.

[7] T. Shimizu, A. Watanabe, M. Ogawara, H. Mori, T. Shirasawa, Isoaspartate formation and neurodegeneration in Alzheimer's disease, Arch. Biochem. Biophys. 381 (2000) 225–234.

[8] A.E. Roher, J.D. Lowenson, S. Clarke, C. Wolkow, R. Wang, R.J. Cotter, I.M. Reardon, H.A. Zürcher-Neely, R.L. Heinrikson, M.J. Ball, B.D. Greenberg, Structural alterations in the peptide backbone of β-amyloid core protein may account for its deposition and stability in Alzheimer's disease, J. Biol. Chem. 268 (1993) 3072–3083.

[9] T.J. Grabowski, H.S. Cho, J.P. Vonsattel, G.W. Rebeck, S.M. Greenberg, Novel amyloid precursor protein mutation in an Iowa family with dementia and severe cerebral amyloid angiopathy, Ann. Neurol. 49 (2001) 697–705.

[10] H. Fukuda, T. Shimizu, M. Nakajima, H. Hori, T. Shirasawa, Synthesis, aggregation, and neurotoxicity of the Alzheimer's Abeta1–42 amyloid peptide and its isoaspartyl isomers, Bioorg. Med. Chem. Lett. 9 (1999) 953–956.

[11] K. Sakai-Kato, M. Naito, N. Utsunomiya-Tate, Racemization of the amyloidal β Asp[1] residue blocks the acceleration of fibril formation caused by racemization of the Asp[23] residue, Biochem. Biophys. Res. Commun. 364 (2007) 464–469.
[12] N.J. Greenfield, Using circular dichroism spectra to estimate protein secondary structure, Nat. Protoc. 1 (2006) 2876–2890.
[13] J. Reed, T.A. Reed, A set of constructed type spectra for the practical estimation of peptide secondary structure from circular dichroism, Anal. Biochem. 254 (1997) 36–40.
[14] G. Bitan, A. Lomakin, D.B. Teplow, Amyloid β-protein oligomerization, J. Biol. Chem. 14 (2001) 35176–35184.
[15] F. Rahimi, P. Malti, G. Bitan, Photo-induced cross-linking of unmodified proteins (PICUP) applied to amyloidogenic peptides, J. Vis. Exp. 23 (2009) 1–3.
[16] N.E. Pryor, M.A. Moss, C.N. Hestekin, Unraveling the early events of amyloid-β protein (Aβ) aggregation: techniques for the determination of Aβ aggregate size, Int. J. Mol. Sci. 13 (2012) 3038–3072.
[17] Y. Cordeiro, L.M.T.R. Lima, M.P.B. Gomes, D. Foguel, J.L. Silva, Modulation of prion protein oligomerization, aggregation, and β-sheet conversion by 4,4′-dianilino-1,1′-binaphthyl-5,5′-sulfonate (bis-ANS), J. Biol. Chem. 279 (2004) 5346–5352.
[18] A.D. Ferrão-Gonzales, B.K. Robbs, V.H. Moreau, A. Ferreira, L. Juliano, A.P. Valente, F.C.L. Almeida, J.L. Silva, D. Foguel, Controlling β-amyloid oligomerization by the use of naphthalene sulfonates, J. Biol. Chem. 280 (2006) 34747–34754.
[19] S.G. Bolder, L.M. Sagis, P. Venema, E. van der Linden, Thioflavin T and birefringence assays to determine the conversion of proteins into fibrils, Langmuir 23 (2007) 4144–4147.
[20] A. Hawe, M. Sutter, W. Jiskoot, Extrinsic fluorescent dyes as tools for protein characterization, Pharm. Res. 25 (2008) 1487–1499.
[21] M. Bucciantini, G. Calloni, F. Chiti, L. Formigli, D. Nosi, C.M. Dobson, M. Stefani, Prefibrillar amyloid protein aggregates share common features of cytotoxicity, J. Biol. Chem. 279 (2004) 31374–31382.
[22] A.L. Lublin, S. Gandy, Amyloid-β oligomers: possible roles as key neurotoxins in Alzheimer's disease, Mt. Sinai J. Med. 77 (2010) 43–49.
[23] M.E. Larson, S.E. Lesné, Soluble Aβ oligomer production and toxicity, J. Neurochem. 120 (2012) 125–139.
[24] K. Murakami, M. Uno, Y. Masuda, T. Shimizu, T. Shirasawa, K. Irie, Isomerization and/or racemization at Asp[23] of Aβ42 do not increase its aggregative ability, neurotoxicity, and radical productivity *in vitro*, Biochem. Biophys. Res. Commun. 366 (2008) 745–751.
[25] Y. Masuda, K. Irie, K. Murakami, H. Ohigashi, R. Ohashi, K. Takegoshi, T. Shimizu, T. Shirasawa, Verification of the turn at position 22 and 23 of the β-amyloid fibrils with Italian mutation using solid-state NMR, Bioorg. Med. Chem. 13 (2005) 6803–6809.
[26] P.N. McFandden, S. Clarke, Methylation at D-aspartyl residues in erythrocytes: possible step in the repair of aged membrane proteins, Proc. Natl. Acad. Sci. USA 79 (1982) 2460–2464.
[27] G. Jung, J. Ryu, J. Heo, S.J. Lee, J.Y. Cho, S. Hong, Protein L-isoaspartyl *O*-methyltransferase inhibits amyloid beta fibrillogenesis *in vitro*, Pharmazie 66 (2011) 529–534.